γ spectroscopy of the ^{96}Y isotope: Searching for the onset of shape coexistence before $N = 60$

Ł. W. Iskra,[1] S. Leoni,[1,2] B. Fornal,[3] C. Michelagnoli,[4] F. Kandzia,[4] N. Mărginean,[5] M. Barani,[1,2] S. Bottoni,[1,2] N. Cieplicka-Oryńczak,[3] G. Colombi,[1,2,4] C. Costache,[5] F. C. L. Crespi,[1,2] J. Dudouet,[6] M. Jentschel,[4] Y. H. Kim,[4] U. Köster,[4] R. Lica,[5] R. Mărginean,[5] C. Mihai,[5] R. E. Mihai,[5] C. R. Nita,[5] S. Pascu,[5] C. Porzio,[1,2] D. Reygadas,[4] E. Ruiz-Martinez,[4] and A. Turturica[5]

[1]*INFN sezione di Milano via Celoria 16, 20133 Milano, Italy*
[2]*Dipartimento di Fisica, Università degli Studi di Milano, I-20133 Milano, Italy*
[3]*Institute of Nuclear Physics, Polish Academy of Sciences, PL-31-342 Kraków, Poland*
[4]*Institut Laue-Langevin (ILL), 71 Avenue des Martyrs, 38042 Grenoble, France*
[5]*Horia Hulubei National Institute of Physics and Nuclear Engineering (IFIN-HH), Bucharest 077125, Romania*
[6]*Université Lyon 1, CNRS/IN2P3, IPN-Lyon, F-69622 Villeurbanne, France*

(Received 30 May 2020; revised 16 June 2020; accepted 25 August 2020; published 18 November 2020)

Medium and high spin states of the ^{96}Y nucleus, located in the shape-coexistence region near $Z = 40$ and $N = 60$, were populated in thermal-neutron-induced fission of ^{233}U and ^{235}U targets, diluted in a scintillator. γ rays were measured with the FIssion Product Prompt γ-ray Spectrometer (FIPPS) high-purity germanium (HPGe) detector array, using double and triple γ-ray coincidence techniques and taking advantage of the efficient fission tag provided by the scintillating target material. A complex level scheme, extending up to 5.2 MeV and including excitations above the 8^+ β-decaying isomer, was investigated, and firm spin and parity assignments were given to a number of states, on the basis of angular correlation analysis and considerations on the γ-decay patterns. While the structures built on the 0^- ground state and the 8^+ isomer show irregular patterns typical for spherical shapes, the (6^+) isomeric state at 1655 keV [with half-life of 181(9) ns], and the rotational band built on it [with spin-parity values between (6^+) and (9^+)], can be explained by Hartree-Fock-Bogoliubov calculations, if an oblate deformation is assumed. This is the first observation of a deformed structure in an $N = 57$ isotone, lying three neutrons away from the $N = 60$ line. An important finding is also the 115-keV transition which connects the (6^+) 181(9)-ns isomer to the β-decaying 8^+ spherical isomer, allowing us to firmly place the latter at 1541 keV excitation energy. This may be relevant for calculations of electron and antineutrino spectra from fission of actinides, for which ^{96}Y is a prominent product.

DOI: 10.1103/PhysRevC.102.054324

I. INTRODUCTION

Atomic nuclei have the remarkable feature of possessing different geometrical configurations, which are energetically similar, yet have very different surface shapes. This phenomenon, called "shape coexistence," arises from the subtle interplay between macroscopic (collective) and microscopic (individual nucleons) effects [1], and occurs in almost all nuclei (see, e.g., Refs. [1–6]). Adding any new information on nuclear shape-coexistence phenomena is important, as it provides guidance to nuclear structure theory which aims at a unified description of atomic nuclei.

The region of the nuclear chart around $Z = 40$ and $N = 60$ is well known for the appearance of fast changes in coexisting nuclear shapes as a function of proton and neutron number, as well as angular momentum. The sudden onset of the ground-state deformation, observed for neutron-rich nuclei in this region, is considered the most pronounced shape change in the nuclear chart. It can be interpreted in terms of the interchange between coexisting spherical and deformed configurations: while in the isotopes with $N < 60$ the former is energetically most favored, for $N \geqslant 60$ the situation is inverted with the deformed structure becoming the lowest in energy [1,7–14]. In recent years, it was also pointed out that this phenomenon has typical characteristics of quantum-phase transitions [15,16]. A question was raised whether the appearance of deformed structures is restricted to the close proximity of $N = 60$, or whether they also reside in lighter isotopes. In this context, the yttrium isotopic chain offers a perfect testing ground: while the ground state of the ^{96}Y nucleus is considered almost spherical, ^{99}Y and ^{100}Y have a strongly deformed ground state. The transitional nucleus ^{98}Y, located between them, is an extraordinary example of shape coexistence, with a spherical ground state and two low-lying isomeric states (i.e., below 500 keV), with prolate deformation [17].

In this work, we focus on ^{96}Y and we search for clear evidence of coexisting deformed structures, which could be expected to appear at higher excitation energies, as compared to ^{98}Y.

In ^{96}Y, earlier investigations established four states with spin-parities 0^- (the ground state), 1^-, 1^+, and 2^-, by studying the β^- decay of ^{96}Sr [18], as shown in Fig. 1. Unambiguous spin-parity assignments were obtained for most of the identified states by using conversion coefficient measurements and $\gamma\gamma(\theta)$ angular correlations. A long 9.6(2)-s, 8^+

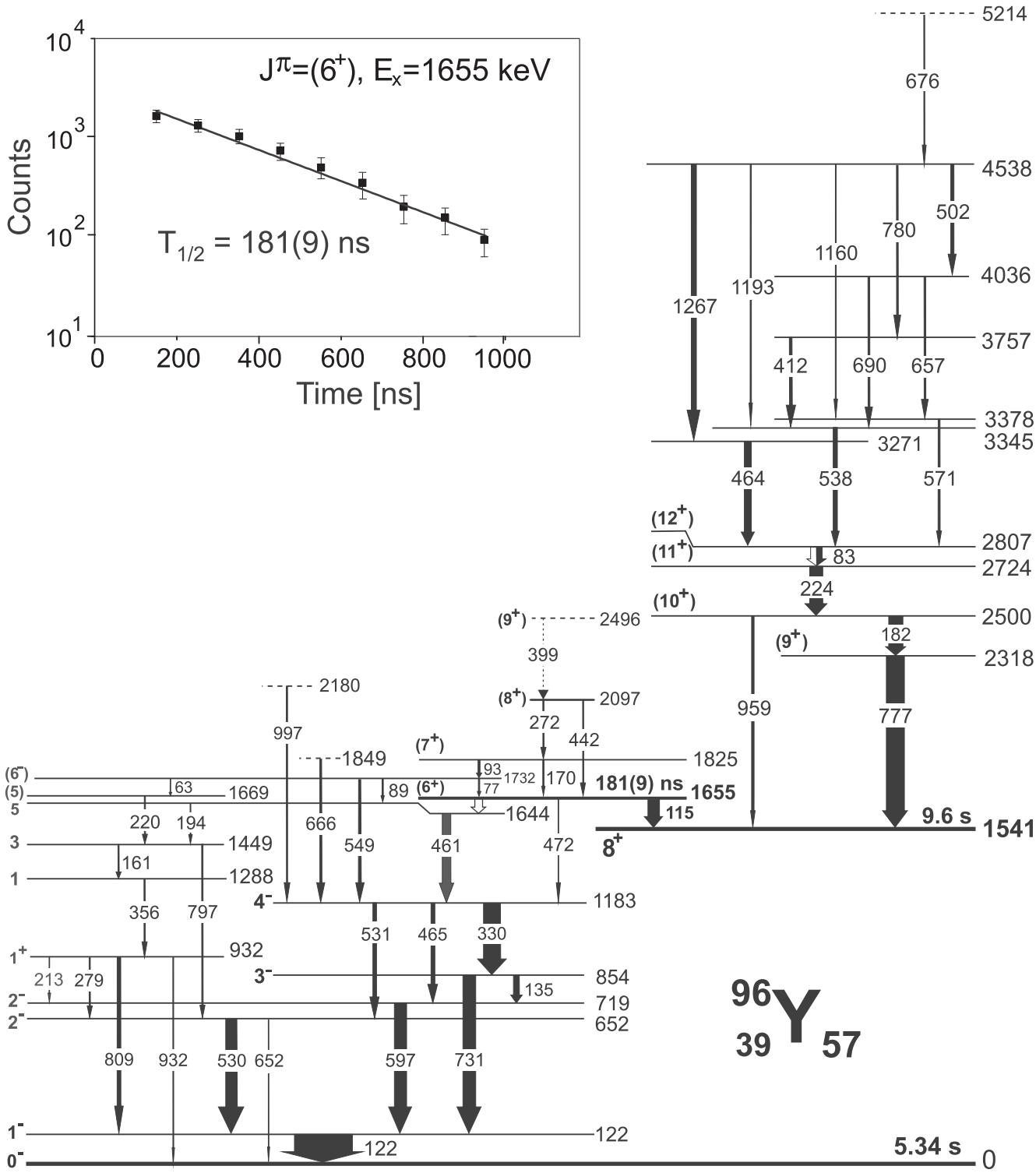

FIG. 1. Level scheme of ^{96}Y, established from the ^{235}U(n, f) and ^{241}Pu(n, f) reactions [22,23] and from the present ^{233,235}U(n, f) studies with the FIPPS array. The arrow widths reflect the observed transition intensities which were obtained with a coincidence time window of 600 ns with respect to the prompt fission event. Inset: intensity of the 461-keV transition, taken in coincidence with the 122-, 330-, and 731-keV lines, as a function of time. It is used to determine the half-life of the isomer located at 1655 keV excitation energy [i.e., $T_{1/2} = 181(9)$ ns].

isomer, β^- decaying to ^{96}Zr, has also been identified and was originally placed at 1140(30) keV in Refs. [19–21], while a later mass measurement located it at 1541(10) keV excitation energy [10].

In our previous works reported in Refs. [22,23], the level scheme of ^{96}Y has been significantly extended by using neutron-induced fission of ^{235}U and ^{241}Pu targets and γ-γ coincidence techniques, taking data from the EXogam@ILL (EXILL) campaign [24]. Yrast and near-yrast states have been located up to about 5.2 MeV of excitation energy, including excitations above the 8^+ long-lived isomer. To most of them, spins and parities were assigned. A new isomeric state at 1655 keV was also observed, with half-life of 201(30) ns. In the present paper, a more detailed γ-spectroscopy analysis for ^{96}Y is reported, based on the high-quality data obtained with the FIPPS array [25] and the active ^{233}U and ^{235}U fissioning targets setup, described in Ref. [26]. In particular, by using the prompt-delayed γ-coincidence technique, a band structure built on the new isomer, at 1655 keV, is firmly established.

II. EXPERIMENTAL PROCEDURES

The data for the present study [27] were obtained by employing the highly efficient high-purity germanium (HPGe) detector array FIPPS (FIssion Product Prompt γ-ray Spectrometer) [25] installed at the Institut Laue-Langevin (ILL) in Grenoble. A collimated thermal neutron beam, with a flux of about 10^8/(s cm^2), induced fission on the ^{235}U and ^{233}U target materials, which were diluted in a deuterated liquid scintillator [26]. Scintillations in the target cell provided precise information on the time of the neutron-induced fission event, giving a clean fission tag. The FIPPS array consisted of eight clover detectors and was supplemented with an additional eight clovers and anti-Compton shields on loan from the IFIN-HH laboratory.

The data were collected in triggerless mode and sorted, during the offline analysis, into two- and three-dimensional histograms, with various time windows. Coincidences between the γ rays were studied using a prompt-prompt (PP) matrix and a prompt-prompt-prompt (PPP) cube, where the γ's were recorded within 150 ns, with respect to the fission event. Also, a delayed-delayed-delayed (DDD) cube was constructed, with a time window of 100–1500 ns, after the fission event. To investigate transitions above the isomer at 1655 keV in ^{96}Y [22], coincidence events were sorted into prompt-prompt-delayed (PPD) and prompt-delayed-delayed (PDD) cubes, where the time condition between γ rays has been optimized for the isomer half-life. In the case of the identification of lines above the long-lived 8^+ isomer, which decays via β^- emission, the technique of cross coincidences has been applied. The method relies on the study of the coincidence relationships with γ rays from the complementary fission fragments. Both the delayed and cross-coincidences techniques are thoroughly described in Refs. [28,29] and in Sec. III of the current work.

For the purpose of angular correlation studies, the FIPPS clover detectors mounted in one ring of octagonal geometry around the target position were used, and the data were sorted considering 21 different angles between the detectors (single crystals of the clover detectors were treated separately). Considering the symmetry with respect to 90°, this resulted in 12 experimental points in the 0°–90° range. The correlations between two γ rays were expressed as a series of Legendre polynomials, i.e., $W(\theta) = \sum A_k P_k(\cos\theta)$, based on the formalism described in Ref. [30]. The experimental A_k coefficients have been compared with theoretical ones in order to test the various hypotheses of multipolarities of the γ rays. The technique was recently applied for the study of the partial level scheme of the ^{96}Y isotope from the EXILL campaign [24] in Refs. [22,23]. In many instances, the analysis provides firm information on spins and parities of intermediate states.

III. EXPERIMENTAL RESULTS

A complex level scheme of ^{96}Y was presented in Refs. [22,23]. Spin-parity assignments to the states lying close to the 0^- ground state and located above the 9.6-s, 8^+ isomer were proposed, on the basis of angular correlations and decay branching considerations. In the present experiment, by employing the active target which provides efficient fission tagging, high-quality spectra of γ transitions, prompt and delayed with respect to the fission event, could be obtained. This allowed us to revisit the spin-parity assignments for selected states, and to expand the level scheme above the 181(9)-ns isomer, located at 1655 keV in Ref. [22]. The full level scheme of ^{96}Y is shown in Fig. 1, while the intensities and energies of all transitions, as well as spin-parity assignments for some of the identified states, are listed in Table I. The results of the angular correlation analysis have been summarized in Table II.

A. The structure near the 0^- ground state

The low-lying structure built on the ground state of the ^{96}Y isotope was investigated using coincidence spectra which were constructed by placing double gates on previously known transitions. For example, a double gate set on the $1^- \rightarrow 0^-$ (ground state) 122-keV and $1^+ \rightarrow 1^-$ 809-keV prompt transitions, as shown in Fig. 2(a), displays the 161-, 220-, and 356-keV lines. Further analysis revealed also the presence of a weak 63-keV transition which deexcites a state at 1732 keV and is in coincidence with the 93- and 220-keV cascade.

Similarly, by setting a double gate on the $1^- \rightarrow 0^-$ 122-keV and the $3^- \rightarrow 1^-$ 731-keV prompt transitions [Fig. 2(b)], γ rays of 89, 93, 272, 330, 461, 549, 666, and 997 keV are seen. Further, a double gate on the $1^- \rightarrow 0^-$ 122-keV and the $5 \rightarrow 4^-$ 461-keV prompt transitions [Fig. 2(c)] shows γ rays located in the bottom part of the level scheme: 135, 465, 530, 531, 597, and 731 keV. We note that in all previously discussed spectra, weak lines of 154, 155, 243, 358, 400, 488, 554, and 621 keV from the ^{137,138}I fission partners (associated with two- and three-neutron evaporation) are observed. Altogether, a detailed analysis of a number of prompt coincidence relationships, constructed from the present FIPPS data, allowed us to confirm the structure near the ground state of ^{96}Y, reported in Ref. [22].

The high-quality FIPPS data were further used to confirm the results of the angular correlation analysis previously reported in Ref. [22]. For example, the pure stretched $E2$ character of the 731-keV transition, connecting states at 854 and 122 keV, has been firmly established [see Fig. 3(a)], pointing to a 3^- assignment for the 854-keV level.

TABLE I. Information on levels and transitions in ^{96}Y from the present experiment. In the first four columns the energies and spin-parities of the initial and final states are given. Column 5 provides the energies of γ rays, while the last column gives relative γ-transition intensities (obtained with a coincidence time window of 600 ns with respect to the prompt fission event), normalized to the 122-keV line (defined as 100 units). Conversion coefficients and multipolarities of transitions are listed in columns 6 and 7 (see also Table II).

E_i (keV)	J_i^π	E_f (keV)	J_f^π	E_γ (keV)	$\alpha(M\lambda, E\lambda)$	Multipolarity	γ Intensity
122.3(1)	1^-	0	0^-	122.3(1)	0.11(2)	$M1$	100
652.3(2)	2^-	122.3(1)	1^-	530.0(1)		$M1+E2$	20.3(35)
		0	0^-	652.3(3)		$E2$	1.4(7)
718.8(2)	2^-	122.3(1)	1^-	596.5(2)		$M1+E2$	21.0(42)
853.5(2)	3^-	718.8(2)	2^-	134.7(1)	0.10(4)	$M1$	11.2(21)
		122.3(1)	1^-	731.2(2)		$E2$	21.7(28)
931.7(2)	1^+	718.8(2)	2^-	213.0(1)		$M1+(E2)$	0.8(2)
		652.3(2)	2^-	279.4(1)		$E1+M2$	1.1(2)
		122.3(1)	1^-	809.4(1)		$E1+(M2)$	7.0(14)
		0	0^-	931.7(1)		$M1+(E2)$	1.6(4)
1183.1(2)	4^-	853.5(2)	3^-	329.6(2)		$M1+E2$	27.3(42)
		718.8(2)	2^-	464.5(2)		$E2$	6.5(6)
		652.3(2)	2^-	531.0(2)		$E2$	4.8(8)
1287.9(3)	1	931.7(2)	1^+	356.2(2)			1.6(3)
1449.3(3)	3	1287.9(3)	1	161.1(2)	0.14(7)		0.7(2)
		652.3(2)	2^-	797.0(2)			2.9(4)
1643.6(2)	5	1449.3(3)	3	194.2(2)			0.4(2)
		1183.1(2)	4^-	460.5(1)			15.4(28)
1655.1(2)	(6^+)	1643.6(2)	5	11.2[a]			[b]
		1540.5(4)	8^+	114.6(3)		$(E2)$	21.2(42)
		1183.1(2)	4^-	472.2(3)		$(M2)$	0.9(3)
1669.0(4)	(5)	1449.3(3)	3	219.7(3)			1.5(4)
1732.2(3)	(6^-)	1669.0(4)	(5)	63.2(5)			0.2(1)
		1655.1(2)	(6^+)	77.1(3)			1.9(3)
		1643.6(2)	5	88.7(2)			1.5(3)
		1183.1(2)	4^-	549.0(2)		$(E2)$	5.0(6)
1824.9(3)	(7^+)	1732.2(3)	(6^-)	92.6(3)		$(M1)$	3.7(5)
		1655.1(2)	(6^+)	169.8(3)		$(M1)$	1.5(3)
1848.8(4)		1183.1(2)	4^-	665.7(3)			3.4(6)
2096.9(5)	(8^+)	1824.9(3)	(7^+)	272.3(3)		$(M1)$	2.2(3)
		1655.1(2)	(6^+)	441.5(3)		$(E2)$	1.8(3)
2179.9(4)		1183.1(2)	4^-	996.8(3)			2.1(3)
2317.9(5)	(9^+)	1540.5(4)	8^+	777.4(2)		$(M1)$	30.1(49)
(2496.1)	(9^+)	2096.9(5)	(8^+)	399.2(5)		$(M1)$	0.9(4)
2499.9(5)	(10^+)	2317.9(5)	(9^+)	182.0(2)	0.04(3)	$(M1+E2)$	24.5(35)
		1540.5(4)	8^+	959.3(3)		$(E2)$	5.2(28)
2724.1(4)	(11^+)	2499.9(5)	(10^+)	224.2(2)		$(M1+E2)$	21.7(35)
2807.1(5)	(12^+)	2724.1(4)	(11^+)	83.0(3)	0.96(23)	$(M1+E2)$	11.9(28)
3271.1(6)		2807.1(5)	(12^+)	464.0(2)			13.3(35)
3345.0(6)		2807.1(5)	(12^+)	537.9(2)			7.7(21)
3378.2(7)		2807.1(5)	(12^+)	571.1(5)			3.5(14)
3757.2(7)		3345.0(6)		412.1(2)			4.2(14)
4035.8(7)		3378.2(7)		657.4(5)			2.1(8)
		3345.0(6)		690.4(5)			2.7(9)
4537.8(5)		4035.8(7)		502.0(2)			5.6(21)
		3757.2(7)		780.3(5)			2.4(8)
		3378.2(7)		1160.1(5)			1.1(6)
		3345.0(6)		1193.0(2)			1.5(6)
		3271.1(6)		1266.7(2)			10.5(14)
5214.0(6)		4537.8(5)		676.2(4)			2.1(8)

[a]From energy difference.

[b]Line not observed. Combining the present intensity analysis with information from PPD and DDD cubes, the total intensity is 6.8(22), which corresponds to 0.80(26) or 0.47(15) γ-ray intensity, assuming $E1$ or $M1$ character, respectively.

TABLE II. Angular correlation results for pairs of transitions in the ^{96}Y isotope together with tentative spin assignments of the considered states. Columns 3 and 4 contain the experimental angular correlation coefficients while the last two columns correspond to the deduced mixing ratios. The bottom part of the table refers to the analysis of angular correlations for cascades above the 8^+, 9.6-s isomer.

E_{γ_1} (keV) - E_{γ_2} (keV)	Spins, $J_i \rightarrow J \rightarrow J_f$	A_2/A_0 (expt.)	A_4/A_0 (expt.)	δ_1	δ_2
597 - 122	$2 \rightarrow 1 \rightarrow 0$	−0.04(4)	0.02(6)	$0.17(^{+5}_{-12})$	0[a]
731 - 122	$3 \rightarrow 1 \rightarrow 0$	−0.7(2)	−0.04(4)	0.00(1)	0[a]
330 - 122[b]	$4 \rightarrow 3; 1 \rightarrow 0$	0.06(2)	0.01(3)	0.00(3)	0[a]
461 - 330	$5 \rightarrow 4 \rightarrow 3$	0.08(2)	0.01(3)	0.00(3)	0
809 - 122	$1 \rightarrow 1 \rightarrow 0$	−0.25(2)	0.00(1)	0.00(1)	0[a]
220 - 809[b]	$(5) \rightarrow 3; 1 \rightarrow 1$	0.12(8)	−0.08(13)	0.0(2)	0[a]
797 - 530	$3 \rightarrow 2 \rightarrow 1$	0.10(2)	0.06(3)	0.00(5)	$-0.11(^{+3}_{-4})$[a]
83 - 224	$(12) \rightarrow (11) \rightarrow (10)$	0.14(4)	−0.06(7)	$0.74(^{+24}_{-19})$	0.28(5)
224 - 182	$(11) \rightarrow (10) \rightarrow (9)$	0.10(4)	0.07(5)	0.28(5)	0.47(13)

[a]From Ref. [18].
[b]Nonconsecutive transitions.

Subsequently, the assignment of 2^- at 719 keV was revisited. As shown in Fig. 3(b), the correlation between the 597- and 122-keV lines strongly points to $\Delta J = 1$ for the 597-keV line, with $M1 + E2$ mixing $\delta = 0.17(^{+5}_{-12})$, which establishes the spin 2 for the 719-keV state. Additionally, $\Delta J = 1$ of the 330-keV transition is confirmed [see Fig. 3(c)], leading to $J = 4$ spin assignment for the 1183-keV level. Yet another support for this scenario is given by the analysis of the conversion coefficient for the 135-keV line between the 854- and 719-keV states. This coefficient was extracted based on the intensity balance of triple coincidence relations with various gating conditions. Only a conversion coefficient associated with an $M1$ dipole transition is in agreement with the 0.10(4) experimental value reported in Table I.

The angular correlations displayed in Fig. 4 support the spin assignments $J = 3$ to the level at 1449 keV, and $J = (5)$ to the 1669 keV level. The $J = 3$ assignment is further confirmed by the conversion coefficient measured for the 161-keV transition, reported in Table I, which points to an $E2$ character.

A $J^\pi = (6^-)$ assignment to the 1732-keV level was suggested in Ref. [22]. Indeed, the decay via the 549-keV transition to the 4^- state excludes the possibility of higher spin value for this state. Also, the $M2$ multipolarity of the 549-keV line is highly unlikely, ruling out the 6^+ spin-parity. Additional support comes from the absence of links to the $J = 3$, 1449-keV and $J^\pi = 3^-$, 854-keV states, which makes the $J < 6$ assignment less likely. The 63-, 77-, and 89-keV branches from the 1732-keV level to the states $J = (5)$ at 1669 keV, the $J^\pi = (6^+)$ isomer at 1655 keV, and $J = 5$ at 1644 keV, are perfectly in line with the (6^-) assignment.

B. The 181(9)-ns isomer and its decay

To investigate the decay of the isomer located at 1655 keV, spectra gated on γ rays delayed with respect to the fission event were constructed from the DDD cube. A spectrum obtained by gating on the delayed 122- and 731-keV transitions, displayed in Fig. 5(a), shows γ rays of energy 330, 461, and 472 keV, belonging to cascades which deexcite the isomer. The 472-keV line, directly deexciting the isomer, is observed in parallel to the 461-keV γ ray from a level at 1644 keV, established earlier, thus confirming the existence of a strongly converted 11-keV isomeric transition. In addition, a double gate on the delayed 530- and 797-keV γ rays, shown in Fig. 5(b), revealed the presence of the 122-keV line, ground-state transition, and of a new 194-keV line, apparently connecting the 1644- and 1449-keV levels. This finding identifies a new way of decay from the isomeric state, at 1655 keV, towards the ground state, involving cascades passing through the 1449-keV level.

The PPD cube was used for a further study of the decay of the isomer located at 1655 keV. Double prompt gates on all possible combinations of the strongest lines located above the isomer were applied, leading to the spectrum shown in Fig. 6. In this spectrum, transitions belonging to cascades deexciting the isomer and earlier observed, i.e., 122-, 330-, 461-, 472-, 530-, 531-, 597-, and 731-keV γ rays, are visible (see Fig. 1). In addition, a new and very strong transition at 115 keV, not present among the cascades deexciting the isomer and feeding the ground state, is clearly observed. By examining the intensity of the 115-keV line with different delayed time windows, the decay curve of the (6^+) isomeric state could be extracted, as shown in the inset of Fig. 6. The half-life $T_{1/2} = 173(15)$ ns of the 1655-keV isomer obtained in this way agrees, within the error, with the value of Ref. [22], and with the refined one based on the full analysis of the present data, as discussed below (see also inset of Fig. 1).

According to the most recent mass measurement study of Hager *et al.* [10], the 9.6-s long-lived 8^+ β-decay isomer is located at 1541(10) keV. In consequence, we propose the 115-keV transition as a link between the 1655-keV isomer and the 8^+ β-decaying state. This placement of the 115-keV γ ray locates the 8^+ isomer precisely at 1540.5(4) keV, which is compatible with the value of Hager *et al.* [10]. A scenario in which the 115-keV line is in cascade with an unobserved low-energy transition is very unlikely: it would require the presence of a $7^{+/-}$ state in close proximity (less than 10 keV) of the (6^+) or 8^+ isomer. One has to note that this finding solves the puzzle of the placement of the 8^+ β-decaying isomer, which was earlier located at 1140(30) keV [21].

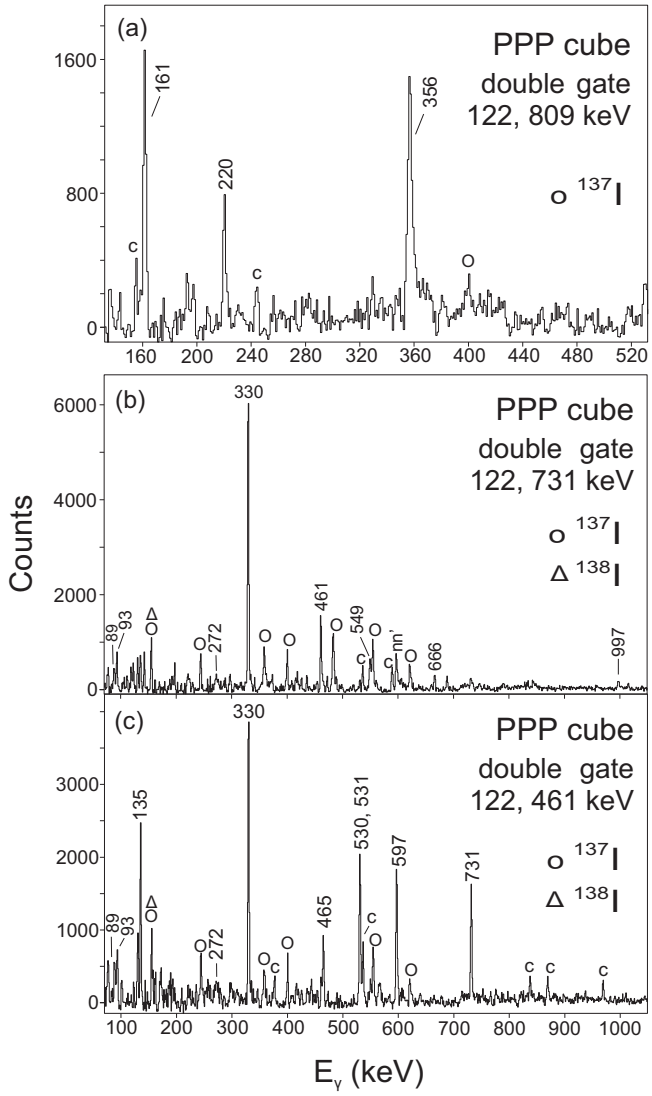

FIG. 2. Coincidence spectra from the PPP cube, used to establish the decay scheme for the structure of ^{96}Y, built on the 0^- ground state. Double gates are placed on γ rays at (a) 122 and 809 keV, (b) 122 and 731 keV, and (c) 122 and 461 keV. Transitions from the ^{137,138}I fission partners are also visible. Contaminants are marked by "c".

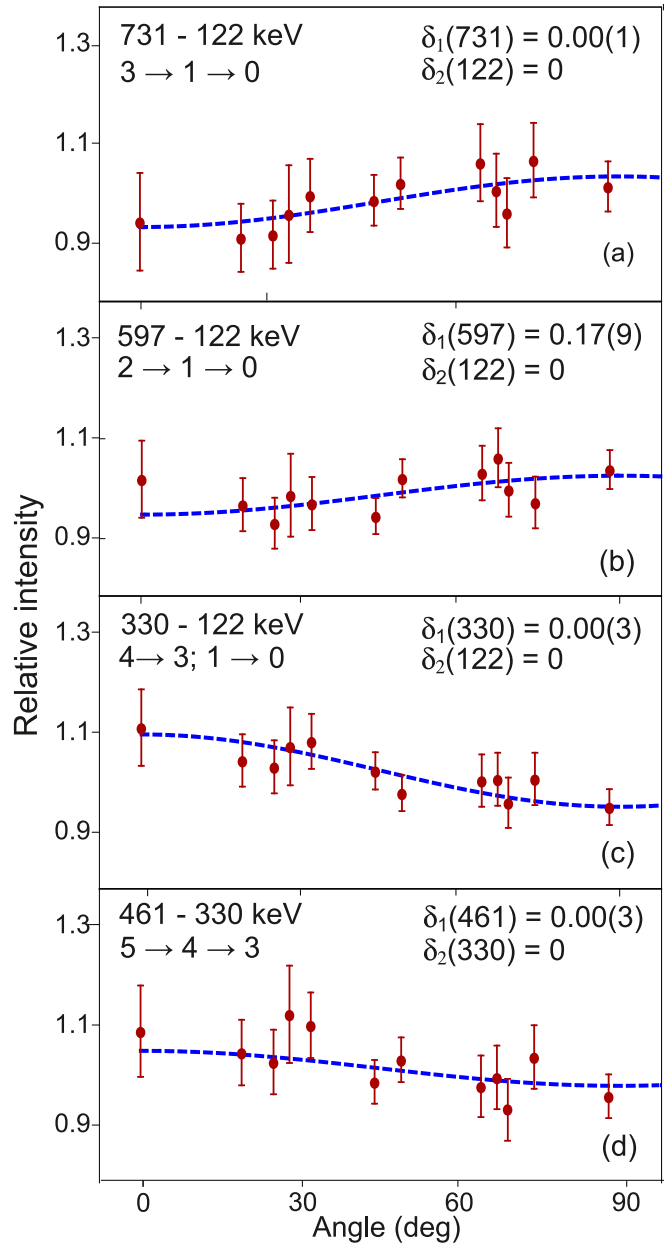

FIG. 3. Experimental γ-γ angular correlations for the selected pairs (a) 731 - 122 keV, (b) 597 - 122 keV, (c) 330 - 122 keV, and (d) 461 - 330 keV of transitions in ^{96}Y. Blue lines are the results of the fitting procedure applied to extract the δ_1 mixing ratio, assuming the spin sequence and the δ_2 fixed value given in the legend (see also Table II). In the case of the 122-keV transition from the first excited 1^- state to the 0^- ground state, a pure $M1$ character was assumed, as reported in Ref. [18].

The efficient fission tag used in the FIPPS array allows a more precise measurement of the half-life of the isomer, located at 1655 keV. To this end, the intensity of the 461-keV line, observed in coincidence with 122-, 330-, and 731-keV lines, was taken at consecutive time intervals with respect to the fission event, and the corresponding decay curve (shown in the inset of Fig. 1) was analyzed. The half-life value of 181(9) ns was obtained, which agrees, within uncertainty, with the previous result of 201(30) ns, reported in Ref. [22].

It was also possible to provide a more precise spin-parity assignment for the 181(9)-ns isomeric state, which in the work of Ref. [22] was proposed to have spin of 5 or 6 $\hbar$ units. The presence of the 115-keV transition linking the 1655-keV isomer to the long-lived 8^+ state provides an additional restriction (see Fig. 1). The assignment of $J = 5$ is rather excluded since it implies an $M3$ or $E3$ character for the 115-keV isomeric transition, which would be in contradiction with the relatively short half-life of the 1655-keV isomer. For the same reason, the 6^- possibility, implying $M2$ multipolarity for the 115-keV γ ray, can be excluded. The remaining option, $J^\pi = (6^+)$, provides a rather satisfactory explanation of the isomeric decay pattern. In this case, a 115-keV branch with $E2$ character competes well with the highly converted

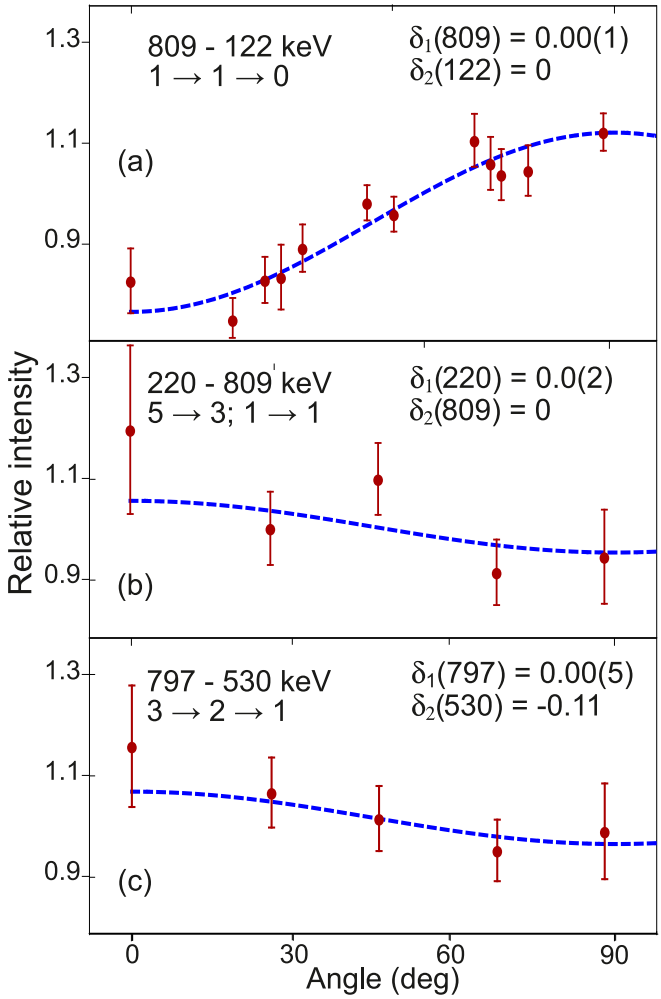

FIG. 4. Experimental γ-γ angular correlations for the pairs (a) 809 - 122 keV, (b) 220 - 809 keV, and (c) 797 - 530 keV, of transitions in ^{96}Y. Blue lines are the results of the fitting procedure applied to extract the δ_1 mixing ratio, assuming the spin sequence and the δ_2 fixed value given in the legend (see also Table II). In the case of the 122-, 530-, and 809-keV transitions, the mixing ratio (δ_2) was taken from Ref. [18].

$\Delta J = 1$ 11-keV transition. Additionally, a much weaker $M2$, 472-keV γ ray can be seen linking the isomer to the 4^- state at 1183 keV. The corresponding reduced transition probabilities are $B(E2) = 3.0(2)$ W.u. and $B(M2) = 7.4(26) \times 10^{-3}$ W.u. for the 115- and 472-keV transitions, respectively. For the unobserved 11-keV transition feeding the 1644-keV state with $J = 5$, both $E1$ and $M1$ multipolarities are possible, leading to $B(E1) = 2.4(8) \times 10^{-5}$ W.u. and $B(M1) = 9.6(30) \times 10^{-4}$ W.u., respectively.

C. The structure above the 181(9)-ns isomer

In this work, we devoted special attention to the investigation of the structure located above the isomeric level at 1655 keV. By setting double coincidence gates, in the PDD cube, on all pairs of 122-, 330-, 461-, 530-, 531-, and 731-keV delayed transitions, γ rays preceding the isomer, with energies

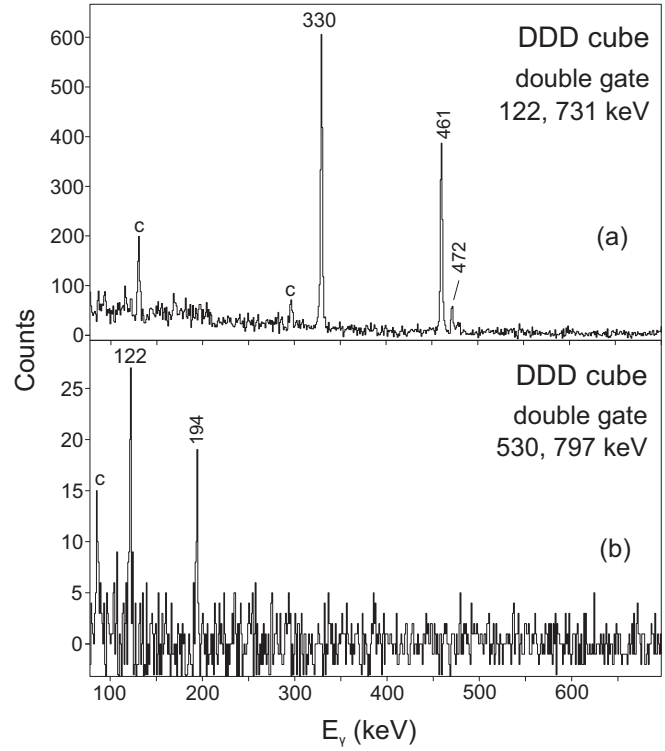

FIG. 5. Coincidence spectra from the DDD cube, used to establish the decay pattern of the 181(9)-ns isomer at 1655 keV. Double gates are placed on γ rays given in the legends. Contaminants are marked by "c".

of 77, 93, 170, 272, and 442 keV reported in the earlier work of Ref. [22], are clearly observed, as shown in Fig. 7. New transitions at 399 and 613 keV can also be recognized as belonging to ^{96}Y. We note that the 93- and 272-keV lines were already seen in the prompt spectra in Figs. 2(b) and 2(c), as transitions feeding the levels at 1183, 1644, and 1669 keV, via the 549-, 89-, and 63-keV transitions, respectively, bypassing the isomer.

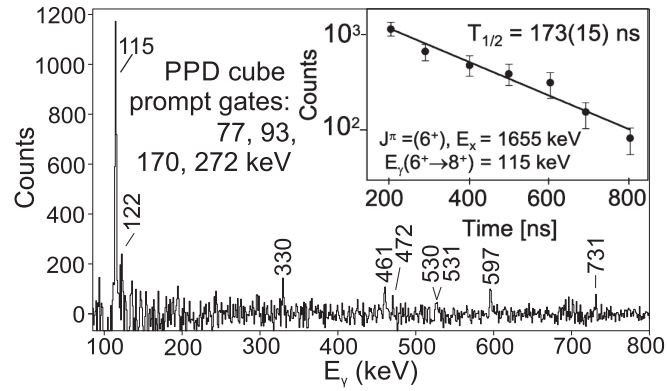

FIG. 6. Delayed spectrum constructed from the PPD cube, setting gates on the most intense pairs of transitions located above the 181(9)-ns isomer. The strongest transitions depopulating the isomer are observed. Inset: decay curve of the 115-keV transition, as extracted from the PPD histogram (see text for details).

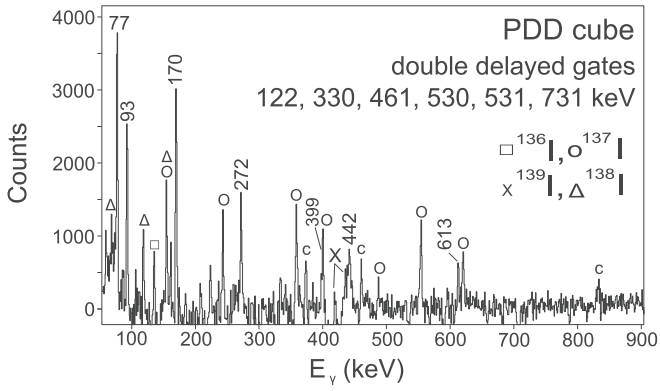

FIG. 7. Prompt spectrum from a PDD cube, used to identify the transitions above the 181(9)-ns isomer at 1655 keV. Double delayed gates are set on transitions located below the isomer, with energies 122, 330, 461, 530, 531, and 731 keV. The strongest transitions from the fission partners are also present. Contaminants are marked by "c".

To locate the newly observed 399- and 613-keV γ rays, we examined the PP coincidence matrix obtained from the PPD cube by setting gates on the 122-, 135-, 330-, 461-, 531-, 597-, and 731-keV transitions located below the 1655-keV isomer. The spectra obtained by requiring prompt gates on the 77-, 93-, and 272-keV lines are shown in Figs. 8(a), 8(b), and 8(c), respectively. The coincidence relations between the 77-, 93-, 170-, and 272-keV transitions confirm the previously established decay pattern, above the isomer. The nonobservation of the 442-keV γ ray is compatible with its placement as being a crossover of the 170- and 272-keV lines, feeding directly the isomer. As shown in Fig. 8(c), a line at 399 keV is also observed in coincidence with the 272-keV transition, which is the most significant in searching for higher-lying transitions, above the 2097-keV state. To get a further insight, we constructed, from the PPD cube, a spectrum gated on the delayed 115-keV and prompt 272-keV transitions; it is shown in Fig. 8(d). Also here, the 399-keV transition appears together with the 77-, 93-, and 170-keV lines. Altogether, we tentatively place the 399-keV γ ray as feeding the 2097-keV state (see Fig. 1). The other 613-keV transition, identified in Fig. 7 as preceding the isomer, could not be firmly placed in the level scheme.

The structure built on the (6^+), 181(9)-ns isomer, at 1655 keV, consists of states at 1825, 2097, and 2496 keV (see Fig. 1). They are connected by a cascade of γ rays with energies of 170, 272, and 399 keV, with the crossover of 442 keV, parallel to the 170- and 272- keV lines. Such arrangement resembles the beginning of a band with $M1$ and $E2$ in-band transitions; therefore, the spin sequence (7^+), (8^+), and (9^+) is tentatively proposed for the states located at 1825, 2097, and 2496 keV, respectively. This structure is similar to the rotational cascade observed in ^{98}Y above the 6.95-μs, 4^- isomeric state [17]. Indeed, as shown in Fig. 9, assuming the proposed spin assignments for the ^{96}Y cascade, the relation between excitation energies and $J(J+1)$ values for the ^{96}Y and ^{98}Y levels above the isomeric states is linear, providing further support for the rotational character of both structures (in red and black, respectively).

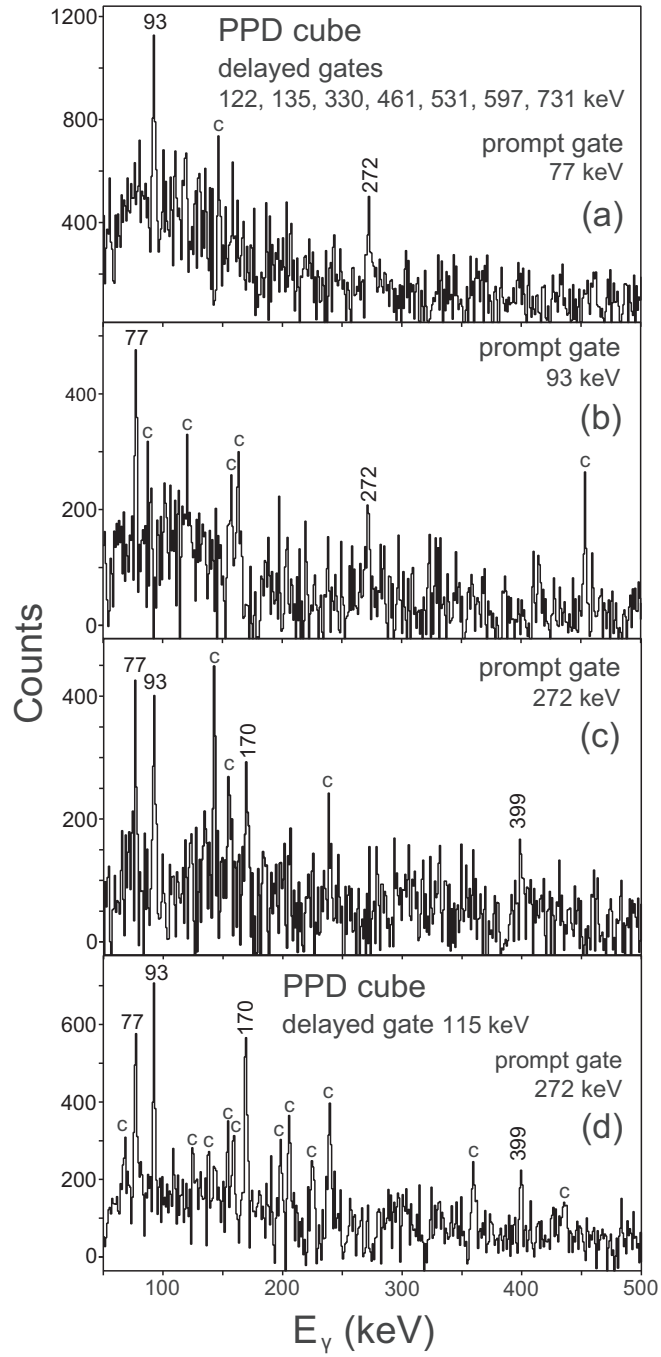

FIG. 8. Prompt spectra constructed from the PPD cube and used to place the transitions located above the 181(9)-ns isomer. Delayed gates are set on the 122-, 135-, 330-, 461-, 531-, 597-, and 731-keV transitions below the isomer. The spectra correspond to prompt gates on the (a) 77-, (b) 93-, and (c) 272-keV transitions, respectively. The spectrum of (d) was obtained by setting gates on the delayed 115-keV and prompt 272-keV transitions. Contaminants are marked by "c".

D. The structure above the long 8^+, 9.6-s isomer

Preliminary identification of the structure built on the 8^+ 9.6-s β-decaying isomer in ^{96}Y, based on results from the EXILL campaign at ILL [24], was reported in Ref. [23]. Here, we confirm the location of this structure, using the superior

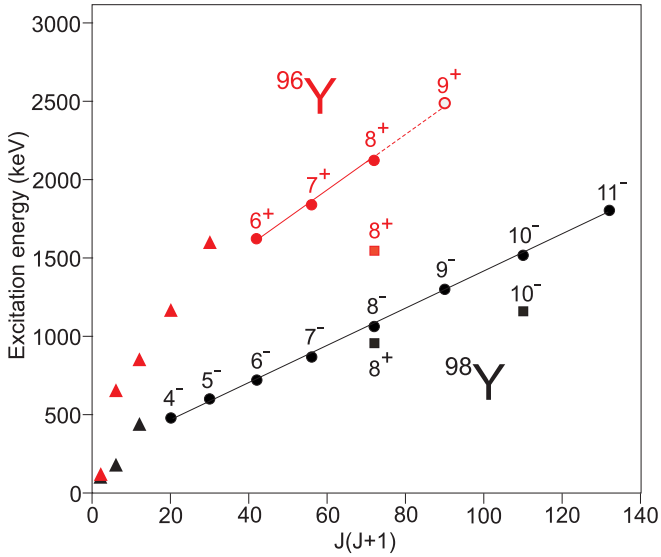

FIG. 9. Excitation energy versus $J(J+1)$ values for the cascades above the 4^- and (6^+) isomers in ^{98}Y (black dots) and ^{96}Y (red dots), respectively. Linear fits are given by straight lines. Squares and triangles indicate spherical isomers and low-spin yrast states, respectively (red for ^{96}Y, black for ^{98}Y).

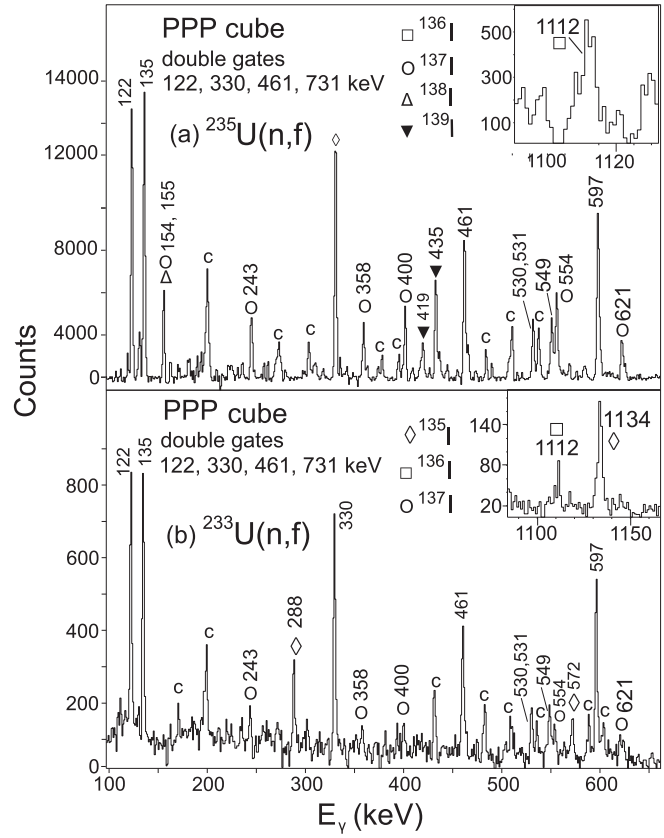

FIG. 10. Coincidence spectra constructed from the PPP cube, by setting double gates on the strongest cascades in the ^{96}Y isotope: (a) the ^{235}U(n,f) reaction, where ^{137}I is the main fission partner of ^{96}Y (three-neutron evaporation channel), and (b) the analogous spectrum for the ^{233}U(n,f) reaction, with ^{135}I as the strongest cross-coincidence partner of ^{96}Y (three-neutron evaporation channel). Contaminants are marked by "c".

data sets obtained with the FIPPS array and thermal-neutron-induced fission on ^{235}U and ^{233}U active targets [26].

The assignment of an unknown sequence of γ rays, not being connected to the known structure in a specific product, may be possible by using the cross-coincidence relationships with transitions in fission reaction partners. In the present work with the ^{233}U and ^{235}U targets, complementary fission products leading to ^{96}Y are iodine nuclei, but ^{96}Y is in coincidence with several I partners because of neutron evaporation from the fission fragments.

The situation is illustrated in Fig. 10(a), which presents the spectrum arising from a sum of double coincidence gates placed on known prompt 122-, 330-, 461-, and 731-keV transitions in ^{96}Y, in the case of the ^{235}U target. This spectrum displays, as expected, known lines from ^{136}I, ^{137}I, ^{138}I, and ^{139}I, which are partners of ^{96}Y associated with four, three, two, and one evaporated neutrons, respectively. A similar spectrum, constructed in the case of the ^{233}U target and shown in Fig. 10(b), presents transitions from ^{135}I, ^{136}I, and ^{137}I, which correspond to three, two, and one evaporated neutrons.

The spectra presented in Figs. 10(a) and 10(b) can be used to estimate the distribution of iodine fragment production yields. To this end, relative intensities of ground-state transitions of I isotopes observed in cross coincidence with the ^{96}Y γ rays were established and are displayed in Figs. 11(a) and 11(e) for ^{235}U and ^{233}U targets, respectively. The intensity pattern of iodine complementary products in the case of both targets indicates that in the fission process up to four neutrons were evaporated, with the $3n$ channel having the largest contribution.

Similar yield distributions of the iodine product complementary to the ^{97}Y and ^{95}Y partners in the case of the ^{235}U and ^{233}U targets are displayed in Figs. 11(c) and 11(d) and Figs. 11(g) and 11(h), respectively. As could be expected, the iodine product intensity distributions are shifted by approximately 1 mass unit toward lower or higher masses for the ^{97}Y and ^{95}Y partners, respectively.

The iodine product intensity pattern obtained by gating on transitions at 182, 224, 464, 777, and 1267 keV, located in Ref. [23] above the 8^+, 9.6-s isomer, are shown in Figs. 11(b) and 11(f) for the ^{235}U and ^{233}U targets, respectively. These intensity distributions resemble very much the product intensity distributions obtained in coincidence with the ^{96}Y γ rays feeding the ground state, thus confirming the identifications done in Ref. [23].

Figure 12(a) shows the spectrum resulting from a prompt double gate on the intense 224- and 777-keV transitions which belong to a cascade which feeds the 8^+ isomer. Clearly visible are the lines at 83, 182, 412, 464, 502, 538, 571, 657, 690, 780, 1160, 1193, and 1267 keV, which were placed in the level scheme above the 8^+ isomer, in the earlier work of Ref. [23]. Figures 12(b)–12(e) display spectra gated on other pairs of prompt γ rays above the isomer. Altogether, the observed coincidence relationships confirm the level scheme proposed in Ref. [23].

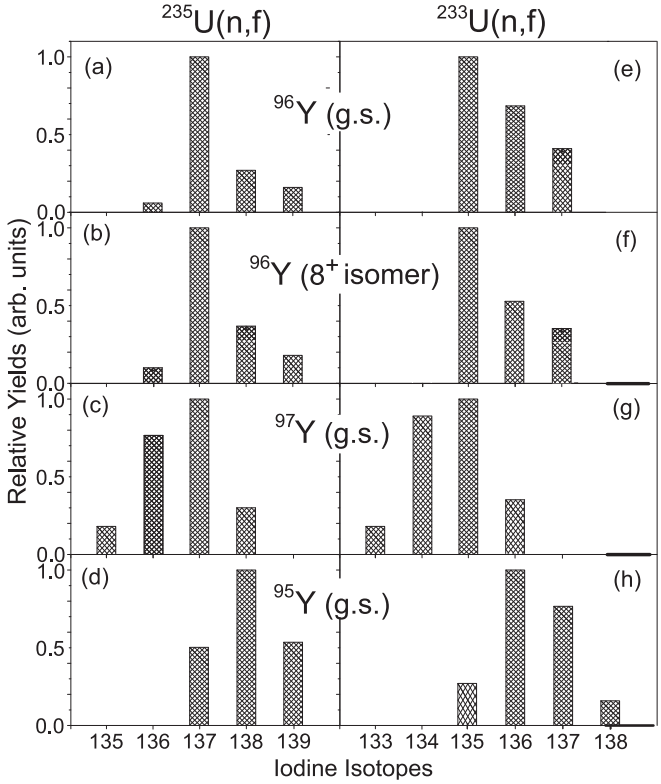

FIG. 11. Relative yields of the cross-coincidence iodine fission partners observed in the ^{235}U(n, f) and ^{233}U(n, f) reactions for ^{96}Y, considering double gates on the prompt 122-, 330-, 461-, and 731-keV lines feeding the 0^- ground state [(a) and (e)] and on the prompt 182-, 224-, 464-, 777-, and 1267-keV γ rays feeding the 8^+ isomer [(b) and (f)]; ^{97}Y, setting double gates on the prompt 792-, 911-, and 990-keV transitions [(c) and (g)]; and ^{95}Y, setting double gates on the prompt 172-, 462-, 969-, and 1086-keV transitions [(d) and (h)].

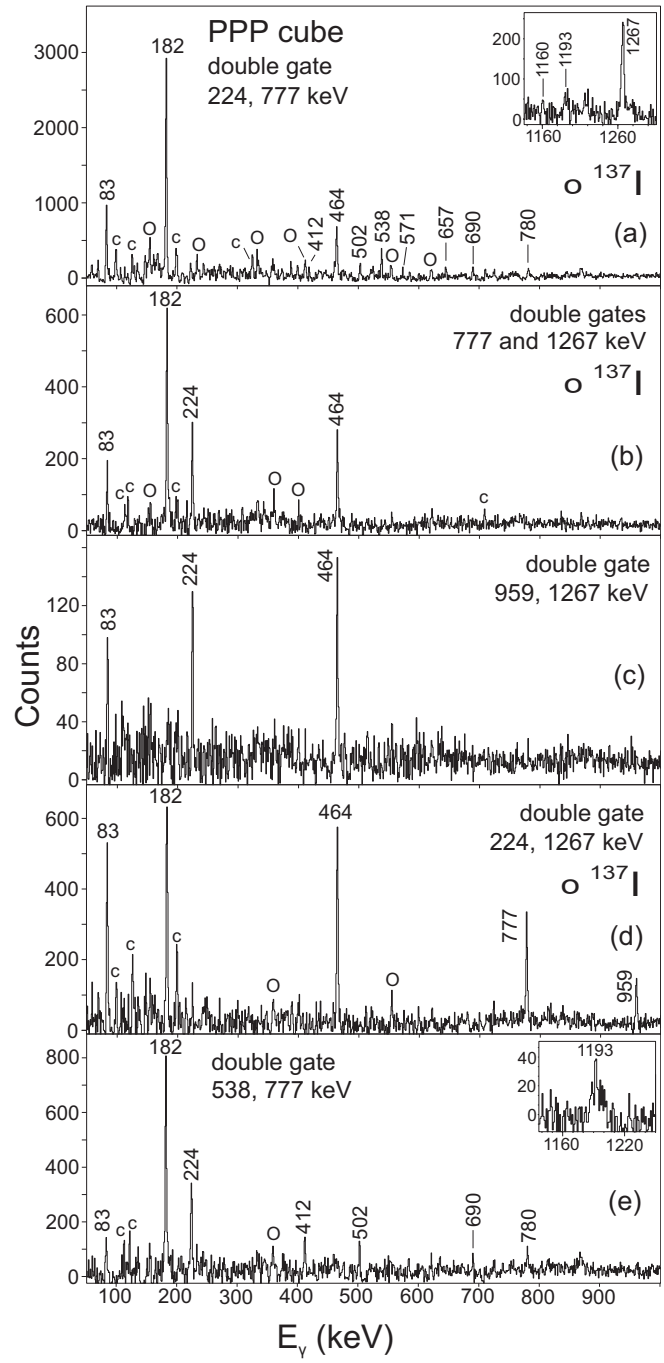

FIG. 12. Prompt coincidence spectra from the PPP cube, used to construct the level scheme above the 9.6-s isomer in the ^{96}Y isotope. Transitions from the most intense ^{137}I fission partner are also observed. Contaminants are marked by "c".

It is remarkable that the structure built on the 8^+, 9.6-s isomer does not appear to be connected to the one built on the ground state of the ^{96}Y isotope, thus pointing to a totally different character of the states involved.

The angular correlation analysis for the structure located above the 8^+ isomer in the ^{96}Y isotope, which was the main part of the work reported in Ref. [23], now is confirmed in the present analysis [see Figs. 13(a) and 13(b)]. Furthermore, it was possible to determine the conversion coefficient for the 83-keV transition, which resulted in the value of 0.96(23). This value points to an $M1 + E2$ character of the 83-keV transition, with a mixing ratio $\delta(83) = 0.74(^{+0.24}_{-0.19})$. Assuming such a mixing, and the spin sequence (9), (10), (11), and (12) for the levels at 2318, 2500, 2724, and 2807 keV, the angular correlation analysis of the pairs 83 - 224 keV and 224 - 182 keV results in the mixing values 0.28(5) and 0.47(13) for the 224- and 182-keV γ rays, respectively. In Sec. IV, these results are discussed in the context of a shell-model approach.

IV. DISCUSSION ON SHAPE COEXISTENCE IN THE ^{96}Y ISOTOPE

Laser spectroscopy studies [11] have clearly shown that in ^{96}Y the 0^- ground state, as well as the 8^+ 9.6-s isomer, have spherical shape. This is in agreement with the conclusions of Ref. [31], where the first excited states were interpreted as shell-model states, arising from the couplings of an unpaired

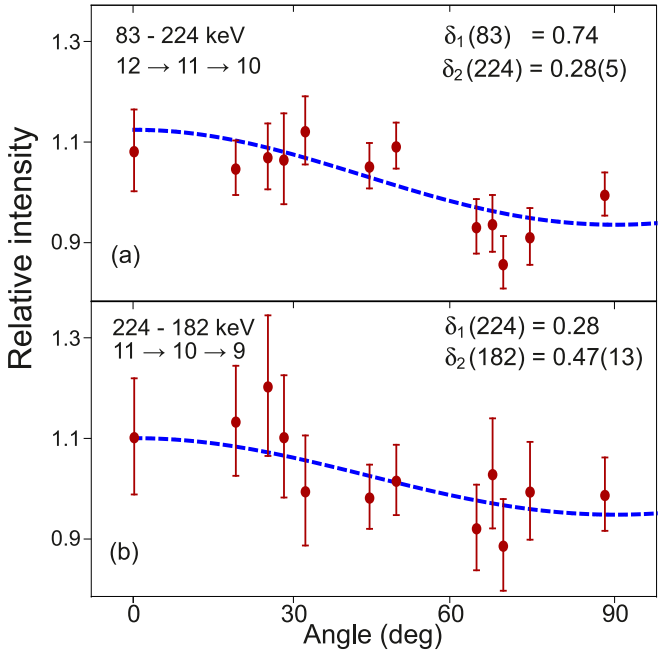

FIG. 13. Experimental γ-γ angular correlations for the pairs (a) 83 - 224 keV and (b) 224 - 182 keV of ^{96}Y. Blue lines are the results of the fitting procedure applied to extract the δ_2 mixing ratios, assuming the spin sequence and the δ_1 fixed value given in the legends (see also Table II).

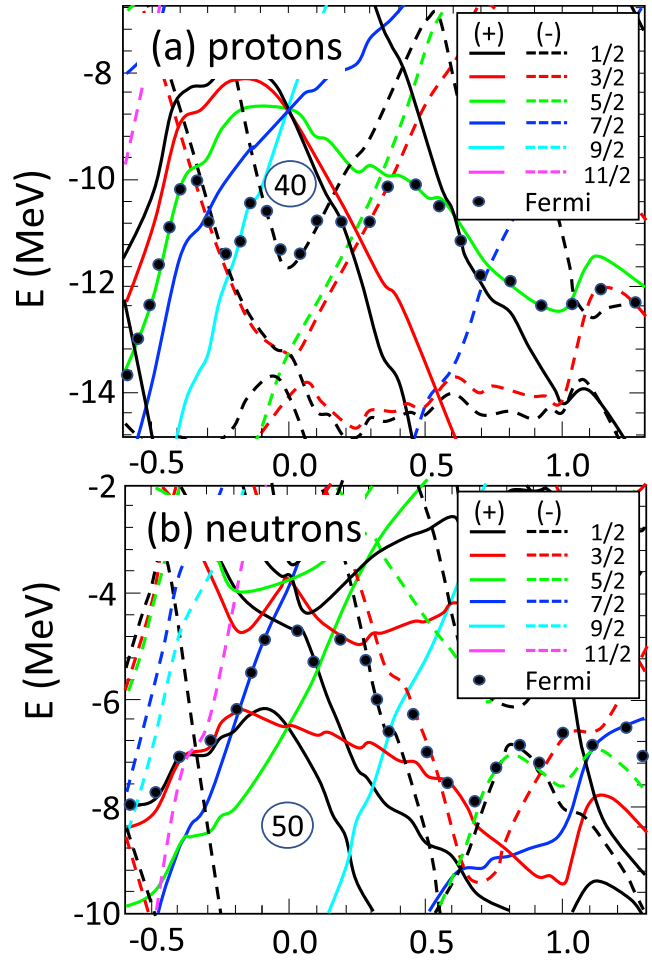

FIG. 14. Single-particle orbitals of ^{96}Y, for (a) protons and (b) neutrons, as follows from Hartree-Fock-Bogoliubov calculations based on the Gogny force. Solid (dashed) lines refer to positive (negative) parity orbitals; black dots indicate the Fermi level (adapted from Refs. [34–36]).

$p_{1/2}$ or $p_{3/2}$ proton with an $s_{1/2}$ or $g_{7/2}$ neutron. Also, in that work the 8^+ isomer was proposed to originate from the maximum spin coupling between the unpaired proton and neutron promoted to the $\pi(g_{9/2})$ and $\nu(g_{7/2})$ orbitals.

A very irregular pattern, observed in our work for the structures built on the 8^+ isomer, supports the shell-model nature of these states. One may speculate about the origin of these high spin states. To obtain spin values larger than 8, one may consider breaking a pair of protons within the proton fp shell; this leads to states with spin-parity up to 11^+. Another way would be to break a neutron pair in the $d_{5/2}$ orbital, promote a neutron to $g_{7/2}$, and decouple the two $g_{7/2}$ neutrons; this produces states with spin-parity up to 13^+. The experimentally observed levels at 2318, 2500, 2724, and 2807 keV, with spin-parities (9^+), (10^+), (11^+), and (12^+), will certainly involve the configurations discussed above.

Apart from the spherical configurations identified in ^{96}Y, the (6^+) isomer and the rotational structure built on it indicate the appearance of deformation in ^{96}Y, at an excitation energy of about 1.6 MeV. This observation may be linked to the general property of nuclei in the region around $Z = 40$ and $N = 60$, where changes in nuclear shape as a function of proton and neutron number, as well as angular momentum, were reported [11–13]. In particular, the coexistence of different shapes in ^{98}Y and ^{99}Y nuclei was established in a series of experiments [17,32,33]. In these nuclei, a prolate-deformed minimum in the nuclear potential arises from the occupation of the "deformation driving" low-Ω subshells of the neutron intruder orbital $\nu h_{11/2}$ and high-Ω subshells of the neutron extruder $\nu g_{9/2}$. For example, in ^{98}Y, a configuration $(\pi 5/2^+[422], \nu 3/2^-[541])4^-$, originating from the $\pi g_{9/2}$ and $\nu h_{11/2}$ orbitals, has been assigned to the deformed 4^- 6.95-μs isomer, at 496 keV. In the same nucleus, the β-decaying (7^+) isomer at 466 keV has been proposed to originate from the $(\pi 5/2^+[422], \nu 9/2^+[404])7^+$ configuration. The same orbitals are responsible for the appearance of the prolate-deformed ground state and isomeric states in ^{99}Y.

In ^{96}Y and ^{97}Y, no collective structures have been identified in earlier works. The band here located above the (6^+) 181(9)-ns isomer is the first manifestation of shape coexistence in an $N = 57$ isotone, lying three neutrons away from the $N = 60$ line.

It is difficult, however, to reconcile the deformed structure observed in ^{96}Y with the collective states known in heavier Y isotopes; in the first approximation one would expect a scenario similar to the one present in ^{98}Y, where the bandheads are 4^- and $(6,7)^+$ [17]. A solution to the question is provided by inspection of the potential energy plot and the deformed single-particle orbital occupation in ^{96}Y given by

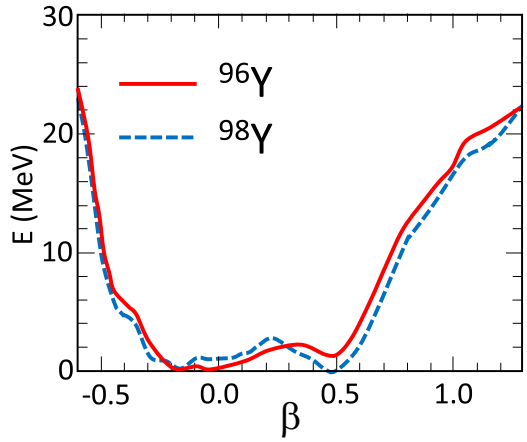

FIG. 15. Potential energy plot for ^{96}Y (red) and ^{98}Y (blue), obtained from Hartree-Fock-Bogoliubov calculations based on the Gogny force (adapted from Refs. [34–36]).

the calculations of Girod and co-workers [34–36], and shown in Figs. 14(a) and 14(b). The calculations predict that in ^{96}Y the oblate minimum lies lower in energy than the prolate one, which is in contrast to the situation in ^{98}Y, as shown in Fig. 15. The (6^+) bandhead of the rotational structure identified in ^{96}Y at 1655 keV requires an energetically favored $K = 6$ coupling. Within the valence space of Fig. 14(a), a good possibility is offered by the oblate $(\pi 9/2^+[404], \nu 3/2^+[411])6^+$ configuration, originating from the the $\pi g_{9/2}$ and $\nu d_{5/2}$ orbitals.

Support for this assignment comes also from the consideration of the moment of inertia, which for the bands in ^{96}Y and ^{98}Y can be estimated from the energy versus spin relation displayed in Fig. 9, as $\approx 25\hbar^2$/MeV and $\approx 50\hbar^2$/MeV, respectively. Indeed, the calculations by Girod and co-workers [34–36] predict for the oblate band in ^{96}Y a value of $\approx 15\hbar^2$/MeV, which is significantly lower than the value of $\approx 35\hbar^2$/MeV expected for the prolate structure in ^{98}Y.

It is worth noting that no transitions connecting the rotational band located in ^{96}Y with the structure identified above the spherical 8^+, 9.6-s isomer have been found, in spite of similar spins of the states involved on both sides. This observation is in line with large structural difference between the two sets of states. It is also very likely that the extension of the rotational band to the higher spin values is limited due to the strong population of the spherical structure located above the long 8^+ isomer, which is yrast in the range of spin values considered here.

V. SUMMARY

Medium and high spin states in the ^{96}Y nucleus, belonging to the shape-coexistence region near $Z = 40$ and $N = 60$, have been populated in thermal-neutron-induced fission of ^{233}U and ^{235}U active targets at ILL, Grenoble. The γ decay of ^{96}Y was studied with the FIPPS array (made of 16 HPGe clovers), using double and triple γ-ray coincidence techniques. The complex level scheme, extending up to 5.2 MeV and including excitations above the 8^+ long-lived isomer, was revisited, and firm spin and parity assignments were given to a number of states on the basis of angular correlation analysis as well as considerations on the γ-decay pattern.

The very irregular patterns observed for the structures built on the 0^- ground state and the 8^+ isomer are in agreement with a shell-model nature of these states and with the laser spectroscopy studies of Cheal *et al.*, which pointed to spherical shapes for both ground and isomeric states.

Of special interest is the isomeric state at 1655 keV, for which a more precise half-life value of 181(9) ns was obtained and spin-parity of (6^+) was assigned. An important finding is the 115-keV transition which connects the isomer to the 9.6-s β-decaying 8^+ spherical isomer. The latter can now be firmly placed at 1541 keV excitation energy, which has to be taken into account in calculations of electron and antineutrino spectra from β-decaying fission products [37,38].

The presence of a rotational structure built on the 181(9)-ns, (6^+) isomer was also firmly established, with spin-parity values between (6^+) and (9^+). The spin (6^+) of the bandhead and the moment of inertia of the band can be explained by the Hartree-Fock-Bogoliubov calculations of Girod and co-workers, if an oblate deformation is assumed. This is the first observation of a deformed structure in an $N = 57$ isotone, lying three neutrons away from the $N = 60$ line. Furthermore, its proposed oblate character differs from the situation in ^{98}Y and heavier yttrium isotopes, where rotational structures coexisting with spherical states are of prolate nature. The appearance of an oblate configuration in ^{96}Y, before prolate structures come into play in heavier Y isotopes, closely resembles the evolution of coexisting spherical-oblate-triaxial-prolate shapes in Zr isotopes with $N = 52$ to $N = 60$, as predicted by Monte Carlo shell-model calculations of Togashi *et al.* [16].

More extensive investigations of the interplay between deformed and spherical structures in other $N = 57$ isotones will become possible by Coulomb excitation and transfer reaction studies with intense postaccelerated radioactive beams, e.g., Sr and Rb, at Isotope Separation On-Line (ISOL) facilities.

ACKNOWLEDGMENTS

This work was supported by the Italian Istituto Nazionale di Fisica Nucleare, by the Polish National Science Centre under Contract No. 2014/14/M/ST2/00738, and by the Romanian UEFISCDI under Contract No. TE 67/2018. The authors acknowledge Gilbert Belier for providing the active target material.

[1] K. Heyde and J. L. Wood, Rev. Mod. Phys. **83**, 1467 (2011).
[2] S. Leoni *et al.*, Phys. Rev. Lett. **118**, 162502 (2017).
[3] N. Mărginean *et al.*, Phys. Rev. Lett. **125**, 102502 (2020).
[4] C. Kremer *et al.*, Phys. Rev. Lett. **117**, 172503 (2016).
[5] P. E. Garrett *et al.*, Phys. Rev. Lett. **123**, 142502 (2019).
[6] A. N. Andreyev *et al.*, Nature **405**, 430 (2000).

[7] E. Cheifetz, R. C. Jared, S. G. Thompson, and J. B. Wilhelmy, Phys. Rev. Lett. **25**, 38 (1970).
[8] P. Federman and S. Pittel, Phys. Lett. B **69**, 385 (1977).
[9] P. Federman and S. Pittel, Phys. Rev. C **20**, 820 (1979).
[10] U. Hager *et al.*, Nucl. Phys. A **793**, 20 (2007).
[11] B. Cheal *et al.*, Phys. Lett. B **645**, 133 (2007).
[12] G. Lhersonneau *et al.*, Phys. Rev. C **49**, 1379 (1994).
[13] W. Urban *et al.*, Nucl. Phys. A **689**, 605 (2001).
[14] J. Skalski, S. Mizutori, and W. Nazarewicz, Nucl. Phys. A **617**, 282 (1997).
[15] R. F. Casten, Prog. Part. Nucl. Phys. **62**, 183 (2009).
[16] T. Togashi, Y. Tsunoda, T. Otsuka, and N. Shimizu, Phys. Rev. Lett. **117**, 172502 (2016).
[17] W. Urban *et al.*, Phys. Rev. C **96**, 044333 (2017).
[18] G. Jung *et al.*, Nucl. Phys. A **352**, 1 (1981).
[19] R. Stippler *et al.*, Z. Phys. A **284**, 95 (1978).
[20] M. L. Stolzenwald, G. Lhersonneau, S. Brant, G. Menzen, and K. Sistemich, Z. Phys. A **327**, 359 (1987).
[21] G. Audi, O. Bersillon, J. Blachot, and A. H. Wapstra, Nucl. Phys. A **729**, 3 (2003).
[22] Ł. W. Iskra *et al.*, Europhys. Lett. **117**, 12001 (2017).
[23] Ł. W. Iskra *et al.*, Acta Phys. Pol. B **48**, 581 (2017).
[24] M. Jentschel *et al.*, J. Instrum. **12**, P11003 (2017).
[25] C. Michelagnoli *et al.*, EPJ Web Conf. **193**, 04009 (2018).
[26] F. Kandzia *et al.*, Eur. Phys. J. A **56**, 207 (2020).
[27] https://doi.org/10.5291/ILL-DATA.3-17-37.
[28] Ł. W. Iskra, R. Broda, R. V. F. Janssens, J. Wrzesiński, B. Szpak, C. J. Chiara, M. P. Carpenter, B. Fornal, N. Hoteling, F. G. Kondev, W. Królas, T. Lauritsen, T. Pawłat, D. Seweryniak, I. Stefanescu, W. B. Walters, and S. Zhu, Phys. Rev. C **89**, 044324 (2014).
[29] Ł. W. Iskra, R. Broda, R. V. F. Janssens, C. J. Chiara, M. P. Carpenter, B. Fornal, N. Hoteling, F. G. Kondev, W. Królas, T. Lauritsen, T. Pawłat, D. Seweryniak, I. Stefanescu, W. B. Walters, J. Wrzesiński, and S. Zhu, Phys. Rev. C **93**, 014303 (2016).
[30] A. J. Ferguson, *Angular Correlation Methods in Gamma-Ray Spectroscopy* (North-Holland, Amsterdam, 1965).
[31] S. Brant, G. Lhersonneau, M. L. Stolzenwald, K. Sistemich, and V. Paar, Z. Phys. A **329**, 301 (1988).
[32] R. A. Meyer *et al.*, Nucl. Phys. A **439**, 510 (1985).
[33] S. Brant, G. Lhersonneau, and K. Sistemich, Phys. Rev. C **69**, 034327 (2004).
[34] S. Hilaire and M. Girod, Eur. Phys. J. A **33**, 237 (2007).
[35] J. F. Berger, M. Girod, and D. Gogny, Comput. Phys. Commun. **63**, 365 (1991).
[36] J. Dechargé and D. Gogny, Phys. Rev. C **21**, 1568 (1980).
[37] L. Hayen, N. Severijns, K. Bodek, D. Rozpedzik, and X. Mougeot, Rev. Mod. Phys. **90**, 015008 (2018)
[38] L. Hayen, J. Kostensalo, N. Severijns, and J. Suhonen, Phys. Rev. C **100**, 054323 (2019).